

Accelerating uplift in the North Atlantic region as an indicator of ice loss

Yan Jiang, Timothy H. Dixon^{*} and Shimon Wdowinski

Vertical motions of the rocky margins of Greenland and Antarctica respond to mass changes of their respective ice sheets^{1,2}. However, these motions can be obscured by episodes of glacial advance or retreat that occurred hundreds to thousands of years ago^{3–6}, which trigger a delayed response because of viscous flow in the underlying mantle. Here we present high-precision global positioning system (GPS) data that describe the vertical motion of the rocky margins of Greenland, Iceland and Svalbard. We focus on vertical accelerations rather than velocities to avoid the confounding effects of past events. Our data show an acceleration of uplift over the past decade that represents an essentially instantaneous, elastic response to the recent accelerated melting of ice throughout the North Atlantic region. Our comparison of the GPS data to models for glacial isostatic adjustment suggests that some parts of western coastal Greenland were experiencing accelerated melting of coastal ice by the late 1990s. Using a simple elastic model, we estimate that western Greenland's ice loss is accelerating at an average rate of $8.7 \pm 3.5 \text{ Gt yr}^{-2}$, whereas the rate for southeastern Greenland—based on limited data—falls at $12.5 \pm 5.5 \text{ Gt yr}^{-2}$.

Inferring long-term trends from short-term measurements is challenging. For processes such as sea level rise or melting of Greenland's ice sheet, decadal, annual or shorter term variability may obscure longer-term signals of interest. Loss of multi-year land ice in North Atlantic islands (Iceland, Svalbard) has been ongoing for most of the twentieth century, presumably in response to global warming^{7,8}. Greenland's recent history is less clear. Significant losses in the past decade have been inferred from satellite measurements of gravity⁹, elevation¹⁰ and marginal ice flow¹¹, although there is some uncertainty about the rate and timing of ice loss^{9,12}.

High-precision vertical GPS data may also indicate changes in continental and local ice mass, as reduced ice load results in crustal uplift^{1–3,13}. However, there are uncertainties in this approach as well. First, the vertical precision of GPS is lower than the horizontal precision; hence, long time series are required to define trends. Second, as with other techniques, annual variation can be large, reflecting (in part) the elastic response of the Earth to time-varying loads associated with summer melting of marginal ice. Third, such measurements can be made only on the rocky margins of ice-covered areas, giving an incomplete picture. Fourth, complex regional variations may exist in the vertical velocity field of ice-covered regions, for reasons unrelated to (or only weakly related to) the current signal of interest. These include crustal response to local, decadal-scale ice fluctuations, and the delayed response of the Earth to retreat of ice sheets since the Last Glacial Maximum $\sim 20,000 \text{ yr ago}$ ^{14–16} and other ice sheet fluctuations, for example, the Little Ice Age within the past few hundred years. Calculating the overall glacial isostatic adjustment (GIA) signal is challenging, as it

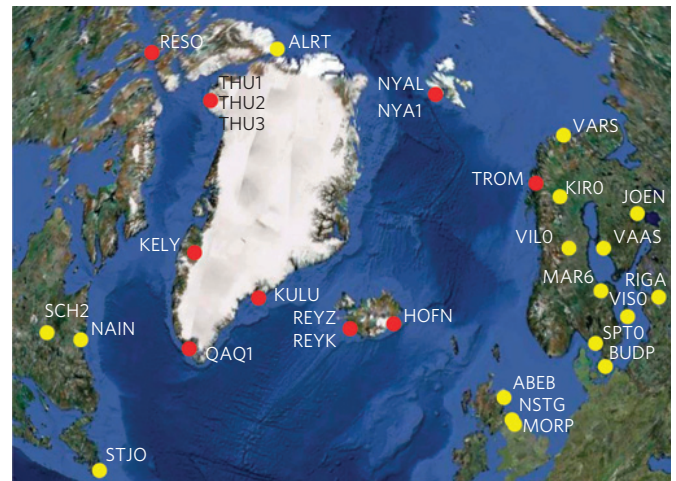


Figure 1 | Location of GPS sites used in this study. The red circles indicate sites with acceleration 0.5 mm yr^{-2} or greater; the yellow circles indicate acceleration less than this value.

depends on the viscosity structure of the mantle and the ice loading history, both of which are uncertain^{15,16}.

We analysed a comprehensive GPS data set to address these problems. Decadal time series with the requisite precision are now available, allowing accurate separation of annual variability from longer term trends. Although we cannot sample vertical crustal motion in the interior of ice-covered regions, existing studies for Greenland^{9–11,17} indicate that high-elevation interior ice is in approximate mass balance. Current mass loss is concentrated in coastal areas, through iceberg calving and summer melting of thin peripheral ice, where GPS stations are located. Regarding the fourth issue (complex vertical velocity field from GIA) we use a new approach, looking at perturbations to velocity rather than the velocity field itself. Results are therefore insensitive to GIA-related vertical motions from past ice mass changes.

We use publicly available data for all North Atlantic regions with significant multi-year land ice (Greenland, Iceland, Svalbard), and adjacent areas (including northeastern Canada and Fennoscandia) for comparison (Fig. 1). We use data sets spanning five years or longer, and simple time series models (Supplementary Information) accounting for equipment changes and annual and semi-annual variation, and either a constant-velocity model (two extra parameters), a constant-acceleration model (three extra parameters) or a 'kink' model, with two velocities and a 'ramp time' (t^*) indicating the time of instantaneous acceleration (four extra parameters; hereafter termed the ramp model). A standard F -test is used to select the appropriate model. Analytical techniques, a results

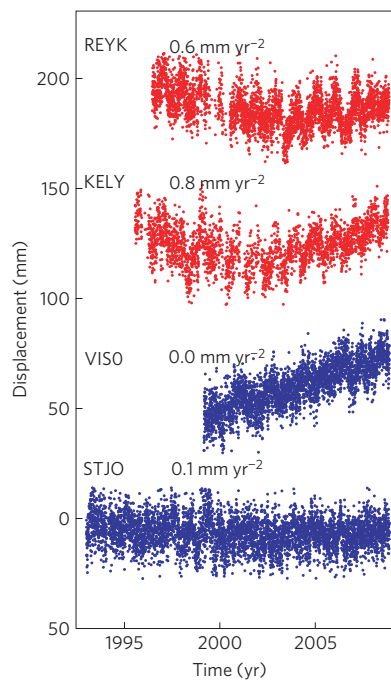


Figure 2 | Representative GPS time series for the North Atlantic region, showing site name and acceleration. The red (upper) time series (Greenland, Iceland) show positive acceleration and the blue (lower) time series (Fennoscandia, Canada) show no significant acceleration; for example, VISO shows uplift at an essentially constant rate. All time series are shown in Supplementary Information.

table and all time series figures are available in Supplementary Information; example time series are shown in Fig. 2. There is a clear difference in the behaviour of Greenland, Iceland and Svalbard sites compared with other sites (Figs 2 and 3). All Greenland, Iceland and Svalbard sites are poorly fitted by a constant-velocity model, exhibiting either significant positive acceleration (constant-acceleration model) or a second phase velocity significantly higher than the first phase velocity (ramp model). Even sites subsiding a decade ago (Supplementary Table S1) are now subsiding less quickly or have begun to uplift. These changes imply significant recent perturbation to mass loading. Although all Greenland sites show positive acceleration, the highest accelerations are recorded at sites for which observations began after 2000, implying that acceleration is recent and ongoing. For Greenland, four of the time series (KELY, THU3, THU2, and the composite time series THUZ) are better fitted by the constant-acceleration model, two sites are marginally better fitted by the ramp model and one site (KULU, in southeast Greenland) is significantly better fitted by the ramp model. The best fit ramp time (t^*) at KULU is 2003.5, coinciding with a period of high summer melting in southeast Greenland¹⁸, and the velocity increase is large, $9 \pm 1 \text{ mm yr}^{-1}$. However, t^* varies widely among remaining Greenland and North Atlantic sites with no obvious pattern and no statistical significance. In the remaining discussion, we focus on the simpler constant-acceleration model (Supplementary Table S1), recognizing that there is extra complexity and information in the time series. In particular, the amplitude of annual uplift, assumed constant in our model, shows significant site-to-site and year-to-year variability, implying sensitivity to local short-term melting and a possible technique for estimating summer mass loss for individual glacier basins¹⁹.

Most remaining sites around the North Atlantic show negligible acceleration, with a mean value (0.04 mm yr^{-2} ; Fig. 3) statistically indistinguishable from zero. Most of these sites are adequately fitted by the simplest (constant velocity) model. These regions have only

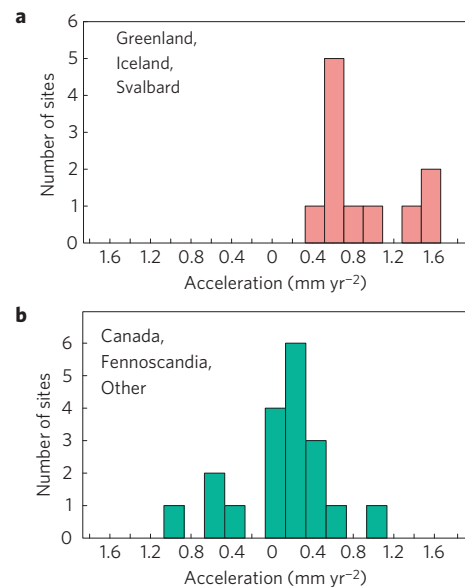


Figure 3 | Histogram of vertical acceleration for GPS sites. a, Areas with significant land ice (Greenland, Iceland, Svalbard) with a mean and standard deviation of 0.87 and 0.46 mm yr^{-2} . **b**, Adjacent North Atlantic areas with only seasonal ice or snow (including northeast Canada and Fennoscandia) with a mean and standard deviation of 0.04 and 0.44 mm yr^{-2} .

seasonal snow and ice, and include sites northwest of Greenland (ALRT), and to the southwest (NAIN), south (STJO), southeast (ABEB, MORP, NSTG) and east (sites in Fennoscandia). These sites experience either steady uplift, presumably related to GIA (refs 20–22) (for example, ABEB, SCH2, most Fennoscandian sites), no significant vertical motion, or slow subsidence (for example, STJO).

With one exception (RESO, possibly influenced by Greenland melting), the only non-Greenland sites experiencing acceleration above 0.5 mm yr^{-2} are in Iceland and Svalbard. Recent melting of Vatnajökull, Iceland's largest glacier, and rapid recent uplift around its margin, have been documented⁷. LaFemina *et al.*²³ document uplift across the whole of Iceland, with uplift increasing linearly towards Vatnajökull, suggesting that most of the island is affected by recent mass reduction of this glacier. HOFN, closest to the glacier, experiences higher acceleration (1.0 mm yr^{-2}) compared with sites near Reykjavik (average 0.5 mm yr^{-2}). Glaciers on Svalbard have been thinning for most of the twentieth century, but increased thinning after 1960 for glaciers in western Svalbard, the location of GPS sites NYA1 and NYAL, has also been documented⁸.

For Greenland, extrapolating the constant-acceleration model to times earlier than 1990 predicts subsidence $> 10 \text{ mm yr}^{-1}$ at most sites, exceeding typical GIA values, suggesting that Greenland's acceleration is a post-1990 phenomenon; that is, the constant-acceleration model cannot apply much earlier than the sample time. Whereas sites near the centre of Laurentide glaciation show uplift at essentially constant velocity, as expected, initial velocities for KELY (southwest Greenland, $-5.3 \pm 0.2 \text{ mm yr}^{-1}$) and THU1 (northwest Greenland, $-1.4 \pm 1.0 \text{ mm yr}^{-1}$) indicate subsidence, similar to some GIA models⁴. More sophisticated (for example, variable acceleration or multiple velocity) vertical motion models and more GPS data could improve such velocity 'hindcasts' to better test GIA models. By 2008, all Greenland sites exhibit rapid uplift (some exceeding 10 mm yr^{-1}), regardless of earlier subsidence.

Vertical motions in Greenland, Iceland and Svalbard reflect both short-term, elastic response to recent ice thinning, and longer term viscous response to past events. However, although velocities are

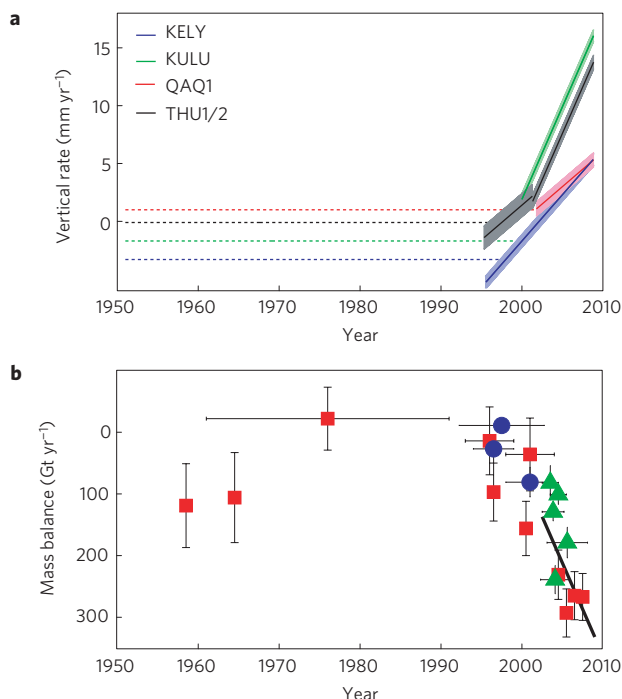


Figure 4 | Rate estimates versus time for Greenland. a, b, Rate estimates versus time for uplift (a) and ice mass balance (b). In a, GPS vertical motions (solid lines, shaded areas indicate uncertainty) are plotted after 1995 assuming constant acceleration model. The dashed lines indicate corresponding GIA estimates⁵. In b, the vertical lines indicate uncertainty; the horizontal lines indicate averaging time³⁰. The blue circles are from altimetry^{10,25}, red squares are from net accumulation/loss^{11,26} and green triangles are from GRACE (refs 9,17). A straight-line (constant acceleration) fit through the mass balance data for the period 1996–2008 has a slope of $-21 \pm 8 \text{ GT yr}^{-2}$. The black line is a constant acceleration GRACE model²⁸.

affected by processes at both timescales, the positive accelerations we observe can reflect only recent events. This is consistent with models of individual glacier changes, where significant elastic response is clearly observable in this type of geodetic data^{18,24}.

Our data are consistent with other observations suggesting accelerated Greenland melting, with some exceptions^{25,26} (Fig. 4). The largest Greenland mass losses reported by the Gravity Recovery and Climate Experiment (GRACE) occurred in summer 2005 and 2007, in coastal southeast and northwest Greenland⁹. Our highest acceleration values (1.6 mm yr^{-2}) are observed in southeast Greenland (KULU, 2000–2008) and northwest Greenland (THU3, 2001–2008).

Figure 4 compares mass balance estimates for Greenland to the GPS vertical data. There is a close correspondence between the overall trend of the mass balance estimates and the GPS time series, both suggesting accelerating ice loss by 2000. GIA estimates for individual locations agree fairly well with GPS velocities until the late 1990s, after which vertical velocities are higher than GIA model predictions. Two western Greenland stations (KELY, THU1) were recording by 1995, providing an estimate of the onset time of accelerated coastal melting at these locations (Supplementary Information). These stations exceed the GIA-predicted value by no later than 1999, similar to the timing of water temperature increases in the Davis Strait and Labrador Sea, and major retreat of western Greenland glaciers (Supplementary Information), as well as increased cumulative melting for Greenland²⁷.

As the crustal response to ice melting observed by GPS is dominantly elastic, and melting is concentrated along the coast, a simple analytical model can be used to relate regional ice loss

and uplift. More detailed models, accounting for annual variation, the change in water loading and the three-dimensionality of the problem, are required for accurate estimates. However, the simple model described here illustrates some important features, and is independent of other techniques except for the observation that ice loss occurs mainly near the coast, where low-elevation ice is present. In western Greenland, satellite imagery (Supplementary Fig. S6) and GRACE (ref. 9) suggest a narrow coastal region of mass loss, from the southern tip of Greenland ($\sim 60^\circ \text{ N}$) to $\sim 75^\circ \text{ N}$. Our data suggest rapid melting to at least 76.5° N (latitude of THU-1,2), a distance of about 1700 km. Satellite images here (Supplementary Fig. S6) suggest that mass loss is confined to a $\sim 30 \text{ km}$ coastal strip, supporting a simple two-dimensional model.

We use an elastic half-space model for calculating surface uplift resulting from ice melt along Greenland's western coast. Using the calculated acceleration values of $0.8\text{--}1.1 \pm 0.1 \text{ mm yr}^{-2}$ (mean 0.9 mm yr^{-2}) we obtain $5 \times 10^7 \text{ N m}^{-1}$ as the load change per year for melting of a 30-km-wide load. Assuming this applies along 1,700 km of western Greenland coast, this is equivalent to an accelerated mass loss of $8.7 \pm 3.5 \text{ GT yr}^{-2}$ for the west coast alone (see the Methods section). We also apply the model to the southeast coast, obtaining $12.5 \pm 7.5 \text{ GT yr}^{-2}$. Our results agree well with a weighted linear fit (equivalent to constant acceleration) through the ice loss data for all of Greenland (Fig. 4) from 1996 onward showing ice loss accelerating at $21 \pm 8 \text{ GT yr}^{-2}$, that is, 0 loss in 1996 to 210 GT yr^{-1} loss in 2006. If we assume the loss begins in 1999, the corresponding value is $30 \pm 17 \text{ GT yr}^{-2}$. A recent GRACE estimate for the period April 2002–February 2009, again for all of Greenland, gives $30 \pm 11 \text{ GT yr}^{-2}$ (ref. 28).

More coastal sites (to obtain regional variation), calibration of the vertical position data for annual ice oscillation (to better constrain material properties), GPS transects perpendicular to the coast (to better estimate load width) and a more realistic three-dimensional model would improve this type of ice mass loss estimate, augmenting space-based monitoring of this ice sheet's health and providing more detailed basin-scale estimates of mass loss than are possible from space.

Methods

Elastic model. We use a simple elastic half-space model for calculating the elastic response of the crust to ice melt along Greenland's coastline. It is a two-dimensional model accounting for surface and subsurface deformation induced by an infinitely long load applied over the half-space's surface along a finite-width strip (2a). We first apply this simple model to western Greenland, because ice loss occurs within a roughly 30-km-wide strip along most of the 1,700-km-long coast (Supplementary Fig. S6). We also applied the model to the southeastern coast, despite the limited data, to obtain an approximate estimate of ice loss in that region; this latter estimate should be interpreted with caution.

Model derivation is based on complex variable methods and can be found in Jaeger *et al.*²⁹ (section 13.4.3). The normal displacement (U) of the surface is

$$U(z=0) = \frac{(1-\nu)N_0}{\pi G(2a)} \times [2a + (x-a)\ln|x-a| - (x+a)\ln|x+a|] + \text{const} \quad (1)$$

where x and z are the horizontal and vertical dimensions, respectively, N_0 is a line load, ν is Poisson's ratio, G is the shear modulus, a is the strip half-width and const is an additive constant derived from a non-dimensional analysis of the logarithmic term. Equation (1) is a modified and corrected form of equation 13.30 in ref. 29, which inadvertently omits the $2a$ term in the denominator. As equation (1) contains an additive constant, it must be solved with respect to a reference point, for example, an undeformed far-field point. The near-field surface displacement with respect to the reference point is

$$U_{x\text{-RP}} = U_x - U_{\text{RP}} = \frac{(1-\nu)N_0}{\pi G(2a)} \times [(x-a)\ln|x-a| - (x+a)\ln|x+a| - (x_{\text{RP}}-a)\ln|x_{\text{RP}}-a| + (x_{\text{RP}}+a)\ln|x_{\text{RP}}+a|] \quad (2)$$

The above equation indicates that for a given GPS station location ($x = x_{\text{GPS}}$), the relations between surface uplift (U) and load change induced by melting ice

(N_0) are linear. We use these relations to calculate the accelerating ice mass loss based on our GPS-derived value of accelerating uplift along Greenland's coastlines. First we rearrange equation (2) to calculate the annual line load change according to each station location and the GPS-derived acceleration

$$N_0(x = x_{\text{GPS}}) = \frac{U_{x-\text{RP}} \pi G (2a)}{(1 - \nu)} \times \frac{1}{((x_{\text{GPS}} - a) \ln|x_{\text{GPS}} - a| - (x_{\text{GPS}} + a) \ln|x_{\text{GPS}} + a| - (x_{\text{RP}} - a) \ln|x_{\text{RP}} - a| + (x_{\text{RP}} + a) \ln|x_{\text{RP}} + a|)} \quad (3)$$

We calculated for each station the annual line load change using a reference far-field point of 400 km, a half strip width (a) of 15 km, a station calculation point 15–65 km from the glacier front and acceptable values for the elastic parameters ($\nu = 0.25$ and $G = 30$ GPa) (Supplementary Table S3). As the values of these parameters are poorly constrained, we solve equation (3) for a range of reasonable parameters yielding an uncertainty range of 30–90% (Supplementary Table S3). Higher uncertainties are found in QAQ1, because of its high acceleration uncertainty. The acceleration values in the two western coast sites (KELY and THUZ) are better determined, leading to better-constrained load change estimates.

The calculated line load changes in KELY and THUZ show very similar values of $5 \times 10^7 \text{ N m}^{-1} \text{ yr}^{-2}$, suggesting that the ice loss is similar along Greenland's entire western coast. It also suggests that our plane strain assumption for the model is justified. Next, we integrate the accelerating load change along the 1,700 km length of Greenland's west coast to obtain an accelerating ice mass loss of $8.7 \pm 3.5 \text{ GT yr}^{-2}$. For the southeastern coast of Greenland, we obtain a single acceleration value for KULU, which has a higher uncertainty level. The high acceleration ($1.6 \pm 0.2 \text{ mm yr}^{-2}$) occurring at a large distance from the ice front (65 km) suggests a much higher ice load change along the southeastern coast. Using the same model, we calculate a line load change of $12.5 \pm 5.5 \times 10^7 \text{ N m}^{-1} \text{ yr}^{-2}$. Integrating this value along the 1,000-km-long Greenland southeastern shoreline, the region of significant ice loss suggested by GRACE (ref. 9), indicates accelerating mass loss here of $12.5 \pm 5.5 \text{ GT yr}^{-2}$.

Received 6 October 2009; accepted 19 March 2010;
published online 16 May 2010

References

- Hager, B. H. Weighing the ice sheets using space geodesy: A way to measure changes in ice sheet mass. *Eos. Trans. AGU* **72** (Spring Meeting Suppl.), 71 (1991).
- James, T. S. & Ivins, E. R. Present-day Antarctic ice mass changes and crustal motion. *Geophys. Res. Lett.* **22**, 973–976 (1995).
- Wahr, J. & Han, D. Predictions of crustal deformation caused by changing polar ice on a viscoelastic earth. *Surv. Geophys.* **18**, 303–312 (1997).
- Tarasov, L. & Peltier, W. R. Greenland glacial history and local geodynamic consequences. *Geophys. J. Int.* **150**, 198–229 (2002).
- Peltier, W. R. Global glacial isostasy and the surface of the Ice-Age Earth: The ICE-5G (VM2) model and GRACE. *Ann. Rev. Earth Planet. Sci.* **32**, 111–114 (2004).
- Fleming, K. & Lambeck, K. Constraints on the Greenland Ice Sheet since the Last Glacial Maximum from sea-level observations and glacial-rebound models. *Quat. Sci. Rev.* **23**, 1053–1077 (2004).
- Pagli, C. *et al.* Glacio-isostatic deformation around the Vatnajökull ice cap, Iceland, induced by recent climate warming: GPS observations and finite element modeling. *J. Geophys. Res.* **112**, B08405 (2007).
- Kohler, J. *et al.* Acceleration in thinning rate on western Svalbard glaciers. *Geophys. Res. Lett.* **34**, L18502 (2007).
- Wouters, B., Chambers, D. & Schrama, E. J. O. GRACE observes small-scale mass loss in Greenland. *Geophys. Res. Lett.* **35**, L20501 (2008).
- Thomas, R., Frederick, E., Krabill, W., Manizade, S. & Martin, C. Progressive increase in ice loss from Greenland. *Geophys. Res. Lett.* **33**, L10503 (2006).
- Rignot, E. & Kanagaratnam, P. Changes in the velocity structure of the Greenland ice sheet. *Science* **311**, 986–990 (2006).
- Rignot, E. & Thomas, R. H. Mass balance of polar ice sheets. *Science* **297**, 1502–1506 (2002).
- Conrad, C. P. & Hager, B. H. The elastic response of the Earth to interannual variations in Antarctic precipitation. *Geophys. Res. Lett.* **22**, 3183–3187 (1995).
- Wahr, J., van Dam, T., Larson, K. M. & Francis, O. Geodetic measurements in Greenland and their implications. *J. Geophys. Res.* **106**, 16567–16582 (2001).
- Khan, S. A. *et al.* Geodetic measurements of postglacial adjustments in Greenland. *J. Geophys. Res.* **113**, B02402 (2008).
- Ivins, E. R. & Wolf, D. Glacial isostatic adjustment: New developments from advanced observing systems and modeling. *J. Geodyn.* **46**, 69–77 (2008).
- Luthcke, S. B. *et al.* Recent Greenland ice mass loss by drainage system from satellite gravity observations. *Science* **314**, 1286–1289 (2006).
- Khan, S. A. *et al.* Elastic uplift in southeast Greenland due to rapid ice mass loss. *Geophys. Res. Lett.* **34**, L21701 (2007).
- Kierulf, H. P., Plag, H.-P. & Kohler, J. Surface deformation induced by present day ice melting in Svalbard. *Geophys. J. Int.* **179**, 1–13 (2009).
- Calais, E., Han, J. Y., DeMets, C. & Nocquet, J. M. Deformation of the North American plate interior from a decade of continuous GPS measurements. *J. Geophys. Res.* **111**, B06402 (2006).
- Sella, G. F. *et al.* Observation of glacial isostatic adjustment in 'stable' North America with GPS. *Geophys. Res. Lett.* **34**, L02306 (2007).
- Milne, G. A. *et al.* Space-geodetic constraints on glacial isostatic adjustment in Fennoscandia. *Science* **291**, 2381–2385 (2001).
- LaFemina, P. C. *et al.* Geodetic GPS measurements in South Iceland: Strain accumulation and partitioning in a propagating ridge system. *J. Geophys. Res.* **110**, B11405 (2005).
- Sauber, J., Plafker, G., Molnia, B. F. & Bryant, M. A. Crustal deformation associated with glacial fluctuations in the eastern Chugach Mountains. *J. Geophys. Res.* **105**, 8055–8077 (2000).
- Zwally, H. J. *et al.* Mass changes of the Greenland and Antarctic ice sheets and shelves and contributions to sea-level rise: 1992–2002. *J. Glaciol.* **51**, 509–527 (2005).
- Hanna, E. *et al.* Runoff and mass balance of the Greenland ice sheet: 1958–2003. *J. Geophys. Res.* **110**, D13108 (2005).
- Van den Broeke, M. *et al.* Partitioning recent Greenland mass loss. *Science* **326**, 984–986 (2009).
- Velicogna, I. Increasing rates of ice mass loss from the Greenland and Antarctic ice sheets revealed by GRACE. *Geophys. Res. Lett.* **36**, L19503 (2009).
- Jaeger, J. C., Cook, N. G. W. & Zimmerman, R. W. *Fundamentals of Rock Mechanics* 4th edn (Blackwell, 2007).
- Alley, R. B., Spencer, M. K. & Anandkrishnan, S. Ice sheet mass balance: Assessment, attribution and prognosis. *Ann. Glaciol.* **46**, 1–7 (2007).

Acknowledgements

We thank R. Alley, S. Anandkrishnan, A. Clement and P. Koons for discussions. The GPS data used in this study are archived at SOPAC and CDDIS, generously made available by a number of national mapping and geodetic authorities including NMA, KMS, FGI, LMV and NRCAN, the Universities of Colorado, Newcastle, Nottingham and Latvia, and other members of IGS. US-funded stations in Greenland are maintained by UNAVCO. This work was supported by grants from ONR, NSF and NASA. Y.J. was supported by a NASA Fellowship.

Author contributions

Y.J. processed the GPS data, conducted the time series analysis and wrote the manuscript. S.W. constructed the elastic model and error analysis. T.H.D. designed the study, did the background research and edited the manuscript.

Additional information

The authors declare no competing financial interests. Supplementary information accompanies this paper on www.nature.com/naturegeoscience. Reprints and permissions information is available online at <http://npg.nature.com/reprintsandpermissions>. Correspondence and requests for materials should be addressed to T.H.D.